LETTER

doi:10.1038/nature10499

A carbon isotope challenge to the snowball Earth

P. Sansjofre[1,2], M. Ader[1], R. I. F. Trindade[2], M. Elie[3]†, J. Lyons[4], P. Cartigny[1] & A. C. R. Nogueira[5]

The snowball Earth hypothesis postulates that the planet was entirely covered by ice for millions of years in the Neoproterozoic era, in a self-enhanced glaciation caused by the high albedo of the ice-covered planet. In a hard-snowball picture, the subsequent rapid unfreezing resulted from an ultra-greenhouse event attributed to the buildup of volcanic carbon dioxide (CO_2) during glaciation[1]. High partial pressures of atmospheric CO_2 (p_{CO_2}; from 20,000 to 90,000 p.p.m.v.) in the aftermath of the Marinoan glaciation (~635 Myr ago) have been inferred from both boron and triple oxygen isotopes[2,3]. These p_{CO_2} values are 50 to 225 times higher than present-day levels. Here, we re-evaluate these estimates using paired carbon isotopic data for carbonate layers that cap Neoproterozoic glacial deposits and are considered to record post-glacial sea level rise[1]. The new data reported here for Brazilian cap carbonates, together with previous ones for time-equivalent units[4–8], provide p_{CO_2} estimates lower than 3,200 p.p.m.v.—and possibly as low as the current value of ~400 p.p.m.v. Our new constraint, and our re-interpretation of the boron and triple oxygen isotope data, provide a completely different picture of the late Neoproterozoic environment, with low atmospheric concentrations of carbon dioxide and oxygen that are inconsistent with a hard-snowball Earth.

Thousands of carbon isotope data have been reported for Neoproterozoic successions in the past decade[4–8], yet the full palaeoenvironmental significance of these data is still largely unappreciated. In particular, coupled carbon isotope data from organic carbon and carbonate have the potential to solve the longstanding conundrum of carbon dioxide concentrations in the aftermath of Neoproterozoic glaciations. This is possible because the difference between the carbon isotope ratio for carbonates ($\delta^{13}C_{carb}$) and that for associated organic matter ($\delta^{13}C_{org}$), $\Delta^{13}C_{carb-org}$, depends strongly on the concentration of dissolved CO_2 in the ocean ($[CO_2]_{aq}$, ref. 9), which can be related to p_{CO_2} (ref. 10). This is illustrated by the decrease of $\Delta^{13}C_{carb-org}$ in the past 20 Myr to today's value of ~22‰ (ref. 9), which accompanied the drawdown of atmospheric p_{CO_2} to the pre-industrial value of 280 p.p.m.v.. In contrast, earlier in the Phanerozoic eon, $\Delta^{13}C_{carb-org}$ mostly remained in the range 28–32‰ (ref. 9), except for brief episodes of lower $\Delta^{13}C_{carb-org}$, such as those reported in the upper Ordovician[11] and at the Permo-Triassic boundary[12].

We obtained paired $\delta^{13}C_{carb}$ and $\delta^{13}C_{org}$ values for post-glacial cap carbonates from western Brazil. Cap carbonates are the stratigraphic horizon marker defining the base of the Ediacaran period (635–542 Myr before present). They were supposedly deposited during the post-glacial sea level rise, in a supersaturated ocean and ultra-greenhouse climate resulting from high atmospheric CO_2 levels following a snowball Earth[1]. The studied cap carbonates come from the southeastern margin of the Amazonian craton, away from the metamorphic Paraguay belt[13]. They form a transgressive systems tract directly above diamictites of the Puga Formation, starting with pink stromatolitic dolostones of the Mirassol d'Oeste Formation (~13 m thick) deposited in shallow oxic waters, overlain by dark grey limestone and shale of the Guia Formation (~50 m thick) deposited below storm wave base. These strata have been correlated to the Marinoan event on the basis of their $\delta^{13}C_{carb}$ of about −5‰, $^{87}Sr/^{86}Sr$ of ~0.7078 and Pb–Pb carbonate age of 627 ± 32 Myr (Fig. 1a; Supplementary Information section 2). The measured $\delta^{13}C_{org}$ values ($n = 29$) are homogeneous, with an average value of −27.3 ± 0.5‰ (Supplementary Table 1). $\delta^{13}C_{carb}$ values are also very homogeneous, averaging −4.8 ± 0.6‰, consistent with previous results on the same unit and on other cap carbonates worldwide (Supplementary Fig. 8). The resulting $\Delta^{13}C_{carb-org}$ values average to 22.7 ± 0.8‰ (Fig. 1a).

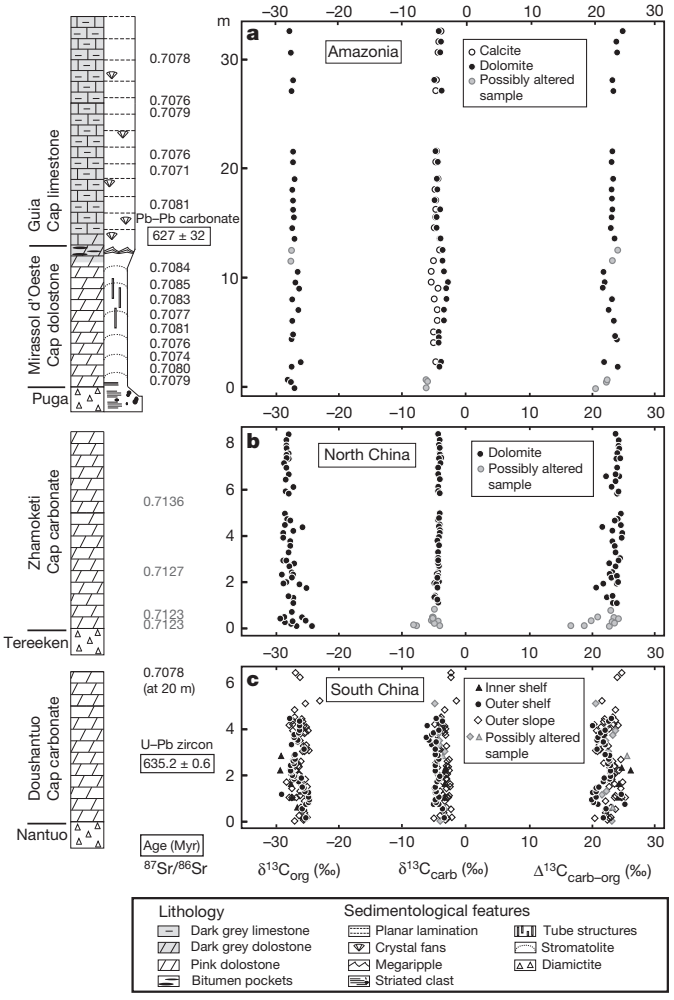

Figure 1 | Isotope and age data for cap carbonates. Paired carbon isotope data ($\delta^{13}C_{org}$ and $\delta^{13}C_{carb}$) for cap carbonate successions from Brazil (Amazonia), North China and South China (this work and refs 4-8), along with geochronological data and $^{87}Sr/^{86}Sr$ ratios (see Supplementary Information sections 2.1 and 2.3 for references). Potentially altered $^{87}Sr/^{86}Sr$ values for Zhamoketi cap dolostones are shown in grey.

[1]Équipe de Géochimie des Isotopes Stables, Institut de Physique du Globe de Paris, Sorbonne Paris Cité, Univ. Paris Diderot, UMR 7154 CNRS, 75238 Paris Cedex 05, France. [2]Departamento de Geofisica, Instituto de Astronomia, Geofísica e Ciências Atmosféricas, Universidade de São Paulo, Rua do Matão 1226, 05508-900 São Paulo, Brazil. [3]UMR CNRS 7566 G2R, Nancy-Université, CNRS, BP 239, 54506 Vandoeuvre-lès-Nancy, France. [4]Institute of Geophysics and Planetary Physics, University of California, Los Angeles, 595 Charles Young Dr. East, Los Angeles, California 90095-1567, USA. [5]Faculdade de Geologia, Instituto de Geociências, Universidade Federal do Pará, CEP 66.075-110, Belém, Brazil. †Present address: Sarawak Shell Berhad Locked Bag No. 1, 98009 Miri, Sarawak, Malaysia.

All other Marinoan cap carbonates for which paired carbon isotope data are available present similarly low $\Delta^{13}C_{carb-org}$ values (Fig. 1). In North China, the 10-m-thick Zhamoketi cap carbonate, deposited above the Tereeken diamictite[4], shows a very stable $\Delta^{13}C_{carb-org}$ signal of 23.6 ± 1.5‰ ($n = 52$, Fig. 1b). In South China, $\Delta^{13}C_{carb-org}$ data for the 3–6-m-thick Doushantuo cap carbonates are available for six sections located along a north–south transect across the Yangtze platform[5–8]. These sections reveal again a low $\Delta^{13}C_{carb-org}$ signal, with an average of 22.7 ± 1.4‰ ($n = 105$, Fig. 1c). Other cap carbonate successions also show systematically low values: the Noonday dolomite, Death Valley (average 19.1 ± 2.7‰, $n = 9$)[14], the Maieberg Formation, Namibia (average 18.7 ± 0.8‰, $n = 8$)[15] and the Tepee dolostone, Western Canada (single value of 22.4‰)[16]. These sections are not considered further, owing to their much smaller data sets.

We have evaluated the extent to which post-depositional processes may have overprinted $\delta^{13}C_{carb}$ (ref. 17) and $\delta^{13}C_{org}$ (ref. 9) in these sections. Available indicators (petrography, Mn/Sr and $\delta^{18}O_{carb}$; Supplementary Information sections 3 and 6, respectively) and the smooth chemostratigraphic trends observed in different successions with similar $\delta^{13}C_{carb}$ (Fig. 1) argue against a significant diagenetic overprint for the $\delta^{13}C_{carb}$ data. As for $\delta^{13}C_{org}$, isotope effects associated with early diagenesis are minor and taken into account in the Δ_2 parameter of equation (1) below (Supplementary Information section 5.1). In addition, molecular organic geochemistry and Rock-Eval pyrolysis data for Brazilian cap carbonates (Supplementary Information section 4) show that the organic matter experienced low thermal maturity and only moderate oxidative weathering, the $\delta^{13}C_{org}$ signal being thus not significantly affected by these processes (Supplementary Information section 5). After screening for post-depositional effects, 26 data (out of 186) were eliminated, and a grand mean $\Delta^{13}C_{carb-org}$ of 23.2 ± 0.9‰ was calculated for the three cap carbonate sequences (Fig. 1). The strong similarity in paired carbon isotope values among the three sequences constitutes the most compelling argument against a first-order diagenetic control on their low $\Delta^{13}C_{carb-org}$.

Anomalous $\Delta^{13}C_{carb-org}$ values in Neoproterozoic successions were previously interpreted as the result of organic matter input from a large dissolved organic carbon (DOC) pool in the ocean[6]. A large DOC reservoir can accumulate only in anoxic waters and would buffer the $\delta^{13}C_{org}$, thus decoupling the $\delta^{13}C_{carb}$ and $\delta^{13}C_{org}$ signals. However, several authors have recently challenged this hypothesis, on the basis of mass balance calculations[6,18]. Moreover, to account for the consistently low $\Delta^{13}C_{carb-org}$ values observed here, cap carbonates must form exclusively in DOC-rich anoxic waters. This contradicts geochemical and magnetic data showing that the basal haematite-bearing cap dolostones were deposited in oxic surface waters[19].

We thus consider that the cap carbonates and associated organic matter originated from the same surface water, so their $\Delta^{13}C_{carb-org}$ can be expressed as[9]

$$\Delta^{13}C_{carb-org} = \varepsilon_p - \Delta_2 + \Delta_{carb} \quad (1)$$

where ε_p is the photosynthetic fractionation factor between dissolved CO_2 and organic matter and depends on $[CO_2]_{aq}$; Δ_2 is the potential increase in $\delta^{13}C_{org}$ during early diagenesis, set here at +1.5‰ (see Methods); and Δ_{carb} is the isotopic depletion of dissolved CO_2 relative to carbonate. Δ_{carb} is temperature-dependent and can be estimated from the carbon isotope fractionation between carbonate species (Methods).

The range of 'normal' ε_p values recorded for most of the Phanerozoic eon[9] (Fig. 2b) matches the low $\Delta^{13}C_{carb-org}$ of cap carbonates ($22.3‰ < \Delta^{13}C_{carb-org} < 24.1‰$) only for temperatures higher than 80 °C. However, the activase of the photosynthetic enzyme (Rubisco) is ineffective above 45 °C (ref. 20), and only non-phototrophic hyperthermophiles can survive in extremely warm environments[21]. As temperatures above 80 °C would be at odds with the presence of

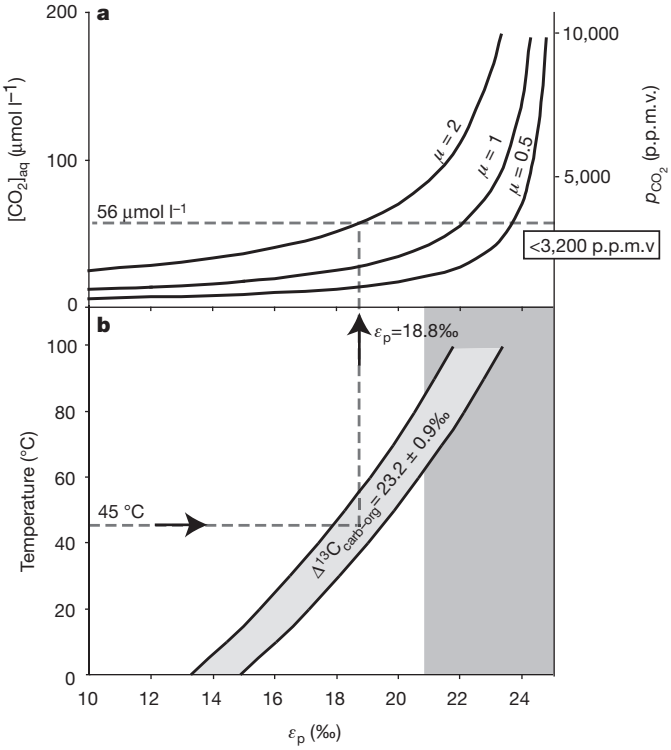

Figure 2 | Relationship between photosynthetic fractionation factor (ε_p), temperature and CO_2 concentrations. **a**, Dissolved CO_2 in the ocean ($[CO_2]_{aq}$) and atmospheric p_{CO_2} versus ε_p for three photosynthesizer growth rates (μ, in d^{-1}), obtained from the relationship $[CO_2]_{aq} = 182\,\mu(V/S)/(25.3\varepsilon_p)$, and assuming chemical equilibrium between ocean and atmosphere. In this equation[27], 25.3‰ is the isotope effect associated with carbon fixation, and the coefficient 182 is partly dependent on cell membrane permeability. **b**, ε_p–T interval compatible with $\Delta^{13}C_{carb-org}$ values of cap carbonates ($22.3 < \Delta^{13}C_{carb-org} < 24.1$‰). At 45 °C, average $\Delta^{13}C_{carb-org}$ implies an ε_p of 18.8‰, and hence a $[CO_2]_{aq}$ of 55.9 μmol l^{-1}, corresponding to an atmospheric p_{CO_2} of 3,200 p.p.m.v.. See text and Methods for details. The shaded area in **b** shows the range of ε_p observed during most of the Phanerozoic eon.

autotroph and heterotroph fossils within and above glacial deposits[22,23] (Supplementary Information section 4), the low $\Delta^{13}C_{carb-org}$ recorded in cap carbonates instead implies low ε_p values (from 18.8‰ at 45 °C to 16.9‰ at 25 °C), similar to those of today[24].

The low ε_p values of cap carbonates are consistent with a low $[CO_2]_{aq}$ during their deposition, regardless of the speciation of carbon (CO_2 or HCO_3^-) and of its uptake mechanism. In some modern settings, ε_p is shifted towards lower values, probably because the system is significantly driven by the active uptake of HCO_3^- (refs 25, 26). But controlled experiments show that the relative contribution of this carbon uptake mechanism decreases significantly as $[CO_2]_{aq}$ increases[25]. For instance, it did not influence ε_p for most of the Phanerozoic, when $[CO_2]_{aq}$ was probably much higher than today[9]. Therefore, this mechanism could account for the systematically low ε_p deduced here only if $[CO_2]_{aq}$ during cap carbonate formation were low—probably below the present-day range of 10–20 μmol kg^{-1}. In the case of dissolved CO_2 uptake, ε_p values can be directly related to $[CO_2]_{aq}$ by empirical equations, which include physiological parameters such as the ratio of cellular volume to surface area, (V/S), and the growth rate (μ) of photosynthesizers. We used the $[CO_2]_{aq}$–ε_p equation from ref. 27 for modern unicellular algal species (Fig. 2a); other equations give similar or lower estimates (see Methods). Figure 2a shows three curves of $[CO_2]_{aq}$ as a function of ε_p for different growth rates and for a V/S of 1 μm. Taking a maximum temperature of 45 °C and a conservative growth rate of 2 d^{-1}, which is rarely attained even in modern high-productivity settings (Supplementary Information section 1), we estimate an absolute $[CO_2]_{aq}$ upper limit of 56 μmol kg^{-1}.

Theoretically, much higher $[CO_2]_{aq}$ values could also produce the low ε_p observed in cap carbonates, but only for extremely high cellular volume and V/S ratios. We note, however, that even if large organisms did flourish just after the glaciation, the increase in cell volume of the biomass would probably be counterbalanced by a large decrease in growth rates. Growth rate and cell volume are related by a power-law, $\mu = aV^b$ (a being a normalization factor and b a size-scaling exponent usually taken as -0.25, ref. 28), which would partly buffer the $[CO_2]_{aq}$ estimates for higher cell volume and consequently for higher V/S ratios (Supplementary Information section 1).

Assuming that atmosphere and ocean are in chemical equilibrium, our $[CO_2]_{aq}$ estimates can be converted into an atmospheric p_{CO_2} of 3,200 p.p.m.v. for the upper estimate ($T = 45\,^{\circ}C$ and $\mu = 2.0\,d^{-1}$) and ~400 p.p.m.v. for a temperature and growth rate similar to present-day values ($T = 25\,^{\circ}C$ and $\mu = 0.5\,d^{-1}$) (Methods). These low p_{CO_2} estimates are in apparent contradiction to the extremely high estimates of 20,000 to 90,000 p.p.m.v. derived from boron isotope[2] ($\delta^{11}B$) and triple oxygen isotope[3] ($\Delta^{17}O$) data. If correct, the whole data set can nonetheless be reconciled into a new environmental picture for the early Ediacaran period.

Boron isotopes, provided that the $\delta^{11}B$ of sea water is known, can be used as a proxy for seawater pH, from which atmospheric p_{CO_2} can be inferred. Kasemann *et al.*[2] have reported a ~4‰ decrease in $\delta^{11}B$ in the Marinoan cap carbonates of the Maieberg Formation (Namibia), which they interpret as resulting from a seawater pH decrease from 8.8 to ≤7, in response to a transfer of CO_2 from a high-p_{CO_2} atmosphere into the surface ocean. As the boron isotopic composition of Neoproterozoic oceans remains unknown, however, only variations in pH can be obtained from $\delta^{11}B$ values[2], not the absolute seawater pH. Therefore, the reported $\delta^{11}B$ decrease is also compatible with low atmospheric p_{CO_2}, assuming a higher seawater pH. This new proposal finds additional support from the global presence of shallow-water marine carbonate in the glacial aftermath, indicating high levels of carbonate saturation, which require elevated seawater pH.

Triple oxygen isotopes measured on sulphates can also be used to constrain atmospheric p_{CO_2} (ref. 3). The acquisition of a negative $\Delta^{17}O$ signature of sulphate occurs in two steps: acquisition of a negative $\Delta^{17}O$ by the oxygen in the atmosphere, followed by transfer of the anomaly to sulphate during oxidative alteration of pyrite in exposed terrestrial sediments. The relationship between p_{CO_2} and $\Delta^{17}O(O_2)$ is given by

$$\Delta^{17}O(O_2) \propto -\Delta^{17}O(CO_{2,trop})\frac{p_{CO_2}}{p_{O_2}}\tau_{O_2} \qquad (2)$$

neglecting multiplicative constants, where $CO_{2,trop}$ is CO_2 crossing the tropopause from the stratosphere, with $\Delta^{17}O(CO_{2,trop}) \approx 1‰$ in the modern atmosphere; and τ_{O_2} is the residence time of O_2 with respect to photosynthesis and respiration (assumed to be in steady state), which is ~1,200 years in the modern atmosphere.

Recently, Bao *et al.*[3] reported a negative $\Delta^{17}O$ anomaly (approximately −0.7‰) in barites intercalated in Marinoan cap carbonates, and interpreted it as a proxy for high atmospheric p_{CO_2}. Abiotic laboratory experiments and experiments with iron-oxidizing organisms have shown that 8–16% of sulphate oxygen is incorporated from atmospheric O_2 (ref. 29), with the remainder from water. Therefore, using a 10% value for atmospheric O_2 incorporation in sulphate, the observed $\Delta^{17}O$(barite) anomaly of −0.7‰ implies a $\Delta^{17}O(O_2)$ of about −7‰. According to equation (2), $\Delta^{17}O(O_2)$ depends on two quantities: p_{CO_2} and the ratio p_{O_2}/τ_{O_2}, which is the photosynthetic O_2 flux. In their model, Bao *et al.*[3] assumed an atmospheric p_{O_2} of ~20% at the end of the Marinoan glaciation, thus resulting in a high p_{CO_2} of ~10,000 p.p.m.v. (Fig. 3, after ref. 3). We interpret these data otherwise, considering lower O_2 fluxes (that is, lower p_{O_2} and/or higher τ_{O_2}), in agreement with available evidence for low p_{O_2} levels in the early Ediacaran (0.2–10%)[30,31]. In such a case, for 1% p_{O_2} and a modern τ_{O_2}, a p_{CO_2} as low as ~ 600 p.p.m.v.—in the range of p_{CO_2} values predicted here from paired carbon isotopic data—would be sufficient to produce the observed $\Delta^{17}O$(barite) of about −0.7‰ (Fig. 3).

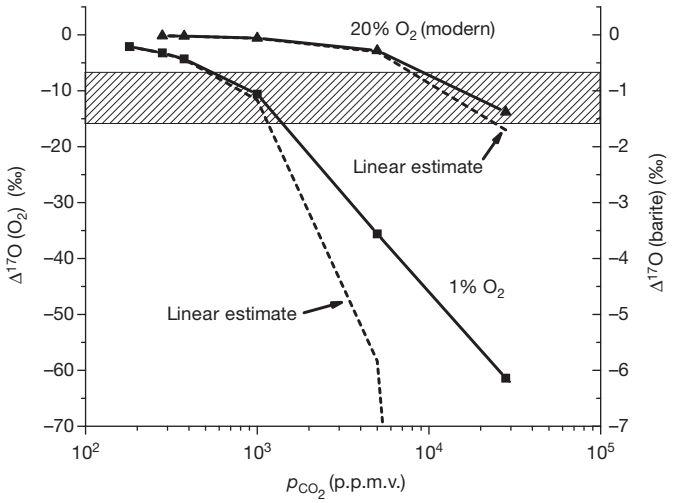

Figure 3 | Relationship between p_{CO_2} (p.p.m.v.) and $\Delta^{17}O(O_2)$ for 20% and 1% O_2, assuming a modern value for O_2 residence time of 1,200 yr. The linear relationship between p_{CO_2} and $\Delta^{17}O(O_2)$ (dashed curves) breaks down for large $\Delta^{17}O(O_2)$ values[3]. The curve for 1% O_2 implies a factor of 20 reduction in the photosynthetic O_2 flux relative to the modern oceanic O_2 flux. The hatched region shows the range of maximum $\Delta^{17}O$ anomalies measured in Marinoan barites and carbonate-associated sulphates (Supplementary Information section 7). Both 1% and 20% O_2 can explain the measured $\Delta^{17}O$, but imply greatly different values for p_{CO_2}.

In conclusion, the low $\Delta^{13}C_{carb-org}$ values reported here for Marinoan cap carbonates not only provide a lower p_{CO_2} estimate than previously thought, but also allow the re-interpretation of $\delta^{11}B$ and $\Delta^{17}O$ isotopic data. The new environmental picture deduced from this integrated interpretation, with low atmospheric p_{CO_2}, high seawater pH and low atmospheric p_{O_2} (associated with low O_2 fluxes), represents a substantial challenge to the hard-end-member snowball Earth picture[1].

METHODS SUMMARY

Samples were ground in an agate mortar, then sieved to ensure a grain size of <140 μm. For carbonate isotope analyses, we used 100% H_3PO_4 to extract CO_2 successively from calcite and dolomite, in a two-step dissolution process (4 h at 25 °C for calcite, then 2 h at 80 °C for dolomite). We measured carbon and oxygen isotope compositions of the evolved CO_2 using a gas chromatograph coupled to a GV Instruments Analytical Precision 2003 mass spectrometer. The external reproducibilities (1σ) for $\delta^{13}C_{carb}$ and $\delta^{18}O_{carb}$ measurements are 0.1‰ and 0.2‰, respectively. For C and N quantification, and organic carbon analysis, samples were decarbonated in 6 N HCl overnight at room temperature, followed by 2 h at 80 °C. Residues were washed with distilled water, centrifuged and dried at 50 °C. Samples of decarbonated powder (10–60 mg) were loaded into quartz tubes along with copper oxide wires. The tubes were connected to a vacuum line and sealed under secondary vacuum ($<10^{-5}$ mbar), then heated at 950 °C for 6 h. The resulting CO_2 and N_2 were purified on a vacuum line and manometrically quantified using a Toepler pump. Total organic carbon content, nitrogen content and hence C/N are deduced from the CO_2 and N_2 quantification with a precision of ±10% relative to the measured value. The carbon isotope composition was measured using a dual-inlet Thermo Finnigan Delta+XP mass spectrometer. The reproducibility of the $\delta^{13}C_{org}$ measurement is ±0.1‰ (1σ). All isotopic results are given in δ notation calibrated to V-PDB (Vienna Pee Dee Belemnite). Rock-Eval analyses and organic geochemistry were performed using standard methods, described in the online Methods section.

Full Methods and any associated references are available in the online version of the paper at www.nature.com/nature.

Received 11 May 2010; accepted 22 August 2011.

1. Hoffman, P. F. & Schrag, D. P. The snowball Earth hypothesis: testing the limits of global change. *Terra Nova* **14,** 129–155 (2002).

2. Kasemann, S. A., Hawkesworth, J. C., Prave, A. R., Fallick, A. E. & Pearson, P. N. Boron and calcium isotope composition in Neoproterozoic carbonate rocks from Namibia: evidence for extreme environmental change. *Earth Planet. Sci. Lett.* **231,** 73–86 (2005).
3. Bao, H., Lyons, J. R. & Zhou, C. Triple oxygen isotope evidence for elevated CO_2 levels after a Neoproterozoic glaciation. *Nature* **453,** 504–506 (2008).
4. Shen, B. *et al.* Stratification and mixing of a post-glacial Neoproterozoic ocean: Evidence from carbon and sulfur isotopes in a cap dolostone from northwest China. *Earth Planet. Sci. Lett.* **265,** 209–228 (2008).
5. McFadden, K. A. *et al.* Pulsed oxidation and biological evolution in the Ediacaran Doushantuo Formation. *Earth Planet. Sci. Lett.* **105,** 3197–3202 (2007).
6. Jiang, G. *et al.* Organic carbon isotope constraints on the dissolved organic carbon (DOC) reservoir at the Cryogenian-Ediacaran transition. *Earth Planet. Sci. Lett.* **299,** 159–168 (2010).
7. Guo, Q. *et al.* Carbon isotopic evolution of the terminal Neoproterozoic and early Cambrian: Evidence from the Yangtze Platform, South China. *Palaeogeogr. Palaeoclimatol. Palaeoecol.* **254,** 140–157 (2007).
8. Ader, M. *et al.* A multilayered water column in the Ediacaran Yangtze platform? Insights from carbonate and organic matter paired $\delta^{13}C$. *Earth Planet. Sci. Lett.* **288,** 213–227 (2009).
9. Hayes, J. M., Strauss, H. & Kaufman, A. J. The abundance of ^{13}C in marine organic matter and isotopic fractionation in the global biogeochemical cycle of carbon during the past 800 Ma. *Chem. Geol.* **161,** 103–125 (1999).
10. Kaufman, A. J. & Xiao, S. High CO_2 levels in the Proterozoic atmosphere estimated from analyses of individual microfossils. *Nature* **425,** 279–282 (2003).
11. Young, S. A., Saltzman, M. R., Bergström, S. M., Leslie, S. A. & Xu, C. Paired $\delta^{13}C_{carb}$ and $\delta^{13}C_{org}$ records of Upper Ordovician (Sandbian-Katian) carbonates in North America and China: Implications for paleoceanographic change. *Palaeogeogr. Palaeoclimatol. Palaeoecol.* **270,** 166–178 (2008).
12. Riccardi, A., Kump, L. R., Arthur, M. A. & D'Hondt, S. Carbon isotopic evidence for chemocline upward excursions during the end-Permian event. *Palaeogeogr. Palaeoclimatol. Palaeoecol.* **248,** 73–81 (2007).
13. de Alvarenga, C. J. S., Santos, R. V. & Dantas, E. L. C-O-Sr isotopic stratigraphy of cap carbonates overlying Marinoan-age glacial diamictites in the Paraguay Belt, Brazil. *Precambr. Res.* **131,** 1–21 (2004).
14. Corsetti, F. A. & Kaufman, A. J. Stratigraphic investigations of carbon isotope anomalies and Neoproterozoic ice ages in Death Valley, California. *Geochim. Cosmochim. Acta* **115,** 916–932 (2003).
15. Kaufman, A. J., Hayes, J. M., Knoll, A. H. & Germs, G. J. B. Isotopic compositions of carbonates and organic carbon from upper Proterozoic successions in Namibia: stratigraphic variation and the effect of diagenesis and metamorphism. *Precambr. Res.* **49,** 301–327 (1991).
16. Narbonne, G. M., Kaufman, A. J. & Knoll, A. H. Integrated chemostratigraphy and biostratigraphy of the Windermere Supergroup, northwestern Canada: Implications for Neoproterozoic correlations and the early evolution of animals. *Geol. Soc. Am. Bull.* **106,** 1281–1292 (1994).
17. Knauth, L. P. & Kennedy, M. J. The late Precambrian greening of the Earth. *Nature* **460,** 728–732 (2009).
18. Bristow, T. F. & Kennedy, M. Carbon isotope excursions and the oxidant budget of the Ediacaran atmosphere and ocean. *Geol. Soc. Am.* **36,** 863–866 (2008).
19. Font, E., Trindade, R. I. F. & Nédélec, A. Detrital remanent magnetization in haematite-bearing Neoproterozoic Puga cap dolostone, Amazon craton: a rock magnetic and SEM study. *Geophys. J. Int.* **163,** 491–500 (2005).
20. Crafts-Brandner, S. J. & Salvucci, M. E. Rubisco activase constrains the photosynthetic potential of leaves at high temperature and CO_2. *Proc. Natl Acad. Sci. USA* **97,** 13430–13435 (2000).
21. Huber, R., Huber, H. & Stetter, K. O. Towards the ecology of hyperthermophiles: biotopes, new isolation strategies and novel metabolic properties. *FEMS Microbiol. Rev.* **24,** 615–623 (2000).
22. Corsetti, F. A., Olcott, A. N. & Bakermans, C. The biotic response to Neoproterozoic snowball Earth. *Palaeogeogr. Palaeoclimatol. Palaeoecol.* **232,** 114–130 (2006).
23. Elie, M., Nogueira, A. C. R., Nédélec, A., Trindade, R. I. F. & Kenig, F. A red algal bloom in the aftermath of the Marinoan snowball Earth. *Terra Nova* **19,** 303–308 (2007).
24. Goericke, R. & Fry, B. Variations of marine plankton $\delta^{13}C$ with latitude, temperature, and dissolved CO_2 in the world ocean. *Glob. Biogeochem. Cycles* **8,** 85–90 (1994).
25. Rost, B., Riebesell, U., Burkhardt, S. & Sültemeyer, D. Carbon acquisition of bloom-forming marine phytoplankton. *Limnol. Oceanogr.* **48,** 55–67 (2003).
26. Werne, J. P. & Hollander, D. J. Balancing supply and demand: controls on carbon isotope fractionation in the Cariaco Basin (Venezuela) Younger Dryas to present. *Mar. Chem.* **92,** 275–293 (2004).
27. Popp, B. N. *et al.* Effect of phytoplankton cell geometry on carbon isotopic fractionation. *Geochim. Cosmochim. Acta* **62,** 69–77 (1998).
28. Finkel, Z. V. *et al.* Phytoplankton in a changing world: cell size and elemental stoichiometry. *J. Plankton Res.* **32,** 119–137 (2010).
29. Balci, N., Shanks, W. C., Mayer, B. & Mandernack, K. W. Oxygen and sulfur isotope systematics of sulfate produced by bacterial and abiotic oxidation of pyrite. *Geochim. Cosmochim. Acta* **71,** 3796–3811 (2007).
30. Rye, R. & Holland, H. D. Paleosols and the evolution of atmospheric oxygen: A critical review. *Am. J. Sci.* **298,** 621–672 (1998).
31. Li, C. *et al.* A stratified redox model for the Ediacaran ocean. *Science* **328,** 80–83 (2010).

Supplementary Information is linked to the online version of the paper at www.nature.com/nature.

Acknowledgements We thank the Geochemistry division of IFP Energie nouvelle for performing Rock-Eval analyses. The work benefited from discussions with M. Bonifacie, G. LeHir, G. Paris and H. Strauss. Research was supported by a French MRT doctoral fellowship and a SETSI grant to P.S., and two INSU (SYSTER) grants to M.A.. R.I.F.T. and A.C.R.N. were supported by the INCT-Geociam programme, and by FAPESP and CNPq grants. J.L. was supported by the NASA Astrobiology Institute under cooperative agreement NNA09DA76 to the Penn State Astrobiology Research Center. This is IPGP contribution 3211.

Author Contributions M.A. and R.I.F.T. conceived the work. P.S., M.A., R.I.F.T. and A.C.R.N. did the sampling. P.S., M.A., R.I.F.T. and P.C. wrote the paper and most of the Supplementary Information. P.S. carried out carbon isotope analyses. P.S. and M.E. did molecular organic geochemistry analyses and wrote the related Supplementary Information. M.A. and M.E. wrote Supplementary Information corresponding to the Rock-Eval data. J.L. performed triple-oxygen modelling and wrote the corresponding parts of the main text and Supplementary Information. A.C.R.N. organized the field work and contributed the geological setting of samples. All authors discussed results and contributed to the manuscript.

Author Information Reprints and permissions information is available at www.nature.com/reprints. The authors declare no competing financial interests. Readers are welcome to comment on the online version of this article at www.nature.com/nature. Correspondence and requests for materials should be addressed to P.S. (sansjofre@ipgp.fr).

METHODS

p_{CO_2} reconstruction. As explained in the main text, ε_p is calculated from $\Delta^{13}C_{carb-org}$, knowing Δ_{carb} and Δ_2 (fixed at 1.5; Supplementary Information section 5.1). Δ_{carb} can be decomposed as the sum of the isotope fractionation factor between carbonate and HCO_3^- ($\Delta^{13}C_{carb-HCO3-}$) and the one between HCO_3^- and CO_{2aq} ($\Delta^{13}C_{HCO3-CO2aq}$). Three sources of $\Delta^{13}C_{carb-HCO3-}$ are available: the $\Delta^{13}C_{CaCO3-HCO3-}$ for inorganic calcite precipitation of 0.9‰ at ambient temperature[32]; the $\Delta^{13}C_{dolomite-HCO3-}$, which ranges from 3.3‰ to 1.2‰ at ambient temperature[33]; and the $\Delta^{13}C_{calcite-HCO3-}$ of −1.2‰, estimated in ref. 9 from the difference between modern carbonate sediments and surface seawater HCO_3^-. We chose this smallest value of $\Delta^{13}C_{CaCO3-HCO3-}$, to ensure that the ultimately derived p_{CO_2} estimate represents an upper limit. Since $\Delta^{13}C_{CaCO3-HCO3-}$ may change slightly with temperature, we used the variation of 0.01‰ °C^{-1} also proposed in ref. 9. In contrast, $\Delta^{13}C_{HCO3-CO2aq}$ is strongly temperature-dependent and is calculated using the formula $\Delta^{13}C_{HCO3-CO2aq} = 9866/(T+273)-24.12$ (ref. 34).

$[CO_2]_{aq}$ is calculated from ε_p using the relation obtained by Popp *et al.*[27] from cultures of unicellular algae (Fig. 2). Other $[CO_2]_{aq}$–ε_p equations have been determined but most of them were obtained for single species at a local scale (in lakes) and do not take into account variations in physiological parameters[35]. Equations based on mixed phytoplankton populations[36,37], which take into account V/S and μ, yield $[CO_2]_{aq}$ estimates inferior to those obtained using Popp *et al.*'s equation. Hence, the choice of this equation provides an upper estimate of $[CO_2]_{aq}$. Moreover, the equation used here is more compatible with the algal signature of molecular organic data (Supplementary Information section 4).

Finally, $[CO_2]_{aq}$ is converted into p_{CO_2}, assuming that ocean and atmosphere were at equilibrium as they are today[24]. Although episodic events of high growth rate can drive the ocean–atmosphere system out of equilibrium owing to the rapid drawdown of ocean CO_2 by photosynthesizers, they are typically local and occur on short timescales. The ubiquitous and homogeneous isotopic record of cap carbonates points instead to a global and persistent process. We used Henry's law: $p_{CO_2} = [CO_2]_{aq}/k_0$. The Henry constant ($k_0$) is expressed as a function of temperature (T) and salinity (S)[38] as follows: $\ln(k_0) = 9345.17/T - 60.2409 + 23.3585\ln(T/100) + S[0.023517 - 0.00023656T + 0.0047036(T/100)^2]$.

We have tested salinity values from 15 to 50 μM (modern value being 35 μM). In the main text, we present only the value corresponding to the highest p_{CO_2} estimate obtained with a high salinity of 50 μM.

Carbon isotope analysis, C and N quantification. Samples were ground in an agate mortar, then sieved to ensure a grain size of <140 μm. Powdered samples were reacted with 100% H_3PO_4 at 25 °C for 4 h to extract the CO_2 from calcite, and then at 80 °C for 2 h to extract CO_2 from dolomite. Carbon and oxygen isotope compositions were measured using a helium continuous flow mass spectrometer (AP 2003). Isotopic compositions are given in the δ notation relative to the V-PDB (Vienna Pee Dee Belemnite). The external reproducibilities (1σ) for $\delta^{13}C_{carb}$ and $\delta^{18}O_{carb}$ measurements are 0.1‰ and 0.2‰, respectively. $\delta^{13}C_{carb}$ values measured on calcite and dolomite were similar, except in the lower part of the dolomite where calcite $\delta^{13}C_{carb}$ values were lower by a maximum of 2‰. Because petrographic observations of these dolostones attest to the secondary character of calcite (Supplementary Information section 3), only the dolomite $\delta^{13}C_{carb}$ values were considered. For C and N quantification, and organic carbon analysis, samples were decarbonated in 6N HCl overnight at room temperature, followed by 2 h at 80 °C. Residues were washed with distilled water, centrifuged and dried at 50 °C. Samples of decarbonated powder (10–60 mg) were loaded into quartz tubes along with copper oxide wires. The tubes were connected to a vacuum line and sealed under secondary vacuum (<10^{-5} mbar), then heated at 950 °C for 6 h. The resulting CO_2 and N_2 were purified on a vacuum line and manometrically quantified using a Toepler pump. Total organic carbon content, nitrogen content and hence C/N are deduced from the CO_2 and N_2 quantification with a precision of ±10% relative to the measured value. The carbon isotope composition was measured using a dual-inlet Thermo Finnigan Delta+XP mass spectrometer at the IPGP, and is expressed in δ notation calibrated to V-PDB (Vienna Pee Dee Belemnite). The reproducibility of the $\delta^{13}C_{org}$ measurement is ±0.1‰ (1σ).

Molecular organic geochemistry. Analyses were performed at Henri-Poincaré University of Nancy. The soluble organic matter was extracted with dichloromethane at 100 bar and 80 °C using an Accelerated Solvent Extractor ASE 200. A blank was performed before each extraction. Two extraction cycles were performed to ensure a complete extraction. Elemental S was removed by introducing HCl activated Cu chips in vials containing the solvent and the extract. Dichloromethane was evaporated using a Zymark TurboVap LV. The extracted organic matter was fractionated into aliphatic and aromatic hydrocarbons on a silica column by successive elution of pentane and pentane/dichloromethane (65/35). Aliphatic hydrocarbons were diluted in hexane (4 mg ml^{-1}) and analysed on a HP5890 Serie II Gas chromatograph coupled with a HP5971 Mass Spectrometer (GC–MS) following the procedure described in ref. 23.

Rock-Eval analyses. Because a TOC content of 0.3% is required for a meaningful determination of Rock-Eval parameters, the bulk-rock organic matter was first concentrated by HF and HCl mineral dissolution using a kerogenatron. Analyses were carried out on the organic concentrate using a Rock-Eval 6 Turbo device at the Institut Français du Pétrole following the classical methodology[39]. The Rock-Eval parameters used were the hydrogen index (HI, mg HC per g TOC) and oxygen index (OI, mg CO_2 per g TOC) also described in ref. 39.

32. Zeebe, R. E. & Wolf-Gladrow, D. CO_2 in *Seawater: Equilibrium, Kinetics, Isotopes* (Elsevier Oceanography Series **65,** (2001).
33. Sheppard, S. & Schwarcz, H. Fractionation of carbon and oxygen isotopes and magnesium between coexisting metamorphic calcite and dolomite. *Contrib. Mineral. Petrol.* **26,** 161–198 (1970).
34. Mook, W. G., Bommerson, C. J. & Staberman, W. H. Carbon isotope fractionation between dissolved bicarbonate and gaseous carbon dioxide. *Earth Planet. Sci. Lett.* **22,** 169–176 (1974).
35. Royer, D. L., Berner, R. A. & Beerling, D. J. Phanerozoic atmospheric CO_2 change: evaluating geochemical and paleobiological approaches. *Earth Sci. Rev.* **54,** 349–392 (2001).
36. Laws, E. A., Popp, B. N., Bidigare, R. R., Kennicutt, M. C. & Macko, S. A. Dependence of phytoplankton carbon isotopic composition on growth rate and $[CO_2]_{aq}$: Theoretical considerations and experimental results. *Geochim. Cosmochim. Acta* **59,** 1131–1138 (1995).
37. Pancost, R. D., Freeman, K. H. & Wakeham, S. G. Controls on the carbon-isotope compositions of compounds in Peru surface waters. *Org. Geochem.* **30,** 319–340 (1999).
38. Weiss, R. F. Carbon dioxide in water and seawater: the solubility of a non-ideal gas. *Mar. Chem.* **2,** 203–215 (1974).
39. Béhar, F., Beaumont, V., De, H. L. & Penteado, B. Rock-Eval 6 technology: performances and developments. *Rev. Inst. Fr. Pet.* **56,** 111–134 (2001).